parity.[20] The magnitude of these values for logft, very little different from those for the transitions to the first excited states, may be explained by the same arguments[18] which apply to the transitions to the first excited states.

The assignment 2− for the ground state of I^{126} is readily interpretable in terms of the nuclear shell model. The only reasonable single-particle configurations[22] which can couple to give the resultant spin-parity value 2− are neutron $h_{11/2}$ and proton $g_{7/2}$.

From the spin and parity assignments for the levels in Xe^{126} and Te^{126} and from the energies of the gamma rays, it is concluded that approximately 1 percent of the total K x-ray intensity from I^{126} arises from internal conversion.[23]

A value, 0.99±0.05 Mev, for the mass difference, Xe^{126} minus Te^{126}, may be calculated from the energies of the ground-state transitions. This figure is believed to be more accurate than that now available from mass measurements.[24]

ACKNOWLEDGMENT

We would like to thank Dr. Rolfe Herber for arranging an irradiation at the MIT cyclotron, and Drs. A. W. Schardt and G. Friedlander for helpful suggestions.

[22] P. F. A. Klinkenberg, Revs. Modern Phys. **24**, 63 (1952).

[23] Rose, Goertzel, Spinrad, Harr, and Strong, Phys. Rev. **83**, 79 (1951).

[24] R. E. Halsted, Phys. Rev. **88**, 666 (1952).

PHYSICAL REVIEW VOLUME 95, NUMBER 1 JULY 1, 1954

Angular Distribution of Charge-Exchange Scattering of 40-Mev π^- Mesons by Hydrogen*

J. TINLOT AND A. ROBERTS
Department of Physics, University of Rochester, Rochester, New York

(Received March 15, 1954)

The angular distribution of the reaction $\pi^-+p\rightarrow\pi^0+n$ has been measured at a mean π^- energy of 40 Mev by detecting coincident photons corresponding to π^0 emission at approximately 0°, 90°, and 180°. The result is

$$d\sigma^0/d\Omega=(0.45\pm0.07)-(0.98\pm0.13)\cos\theta+(0.54\pm0.21)\cos^2\theta \text{ mb/sterad.}$$

The corresponding total cross section is $\sigma_t^0=7.9\pm1.8$ mb. An analysis of this result and of previous measurements on π^+ and π^- scattering at 37 Mev has been made, following the hypothesis of charge independence. It is possible to find two distinct types of solution. One type has positive $T=\frac{1}{2}$ s-wave and $T=\frac{3}{2}$ p-wave phase shifts, and negative $T=\frac{3}{2}$ s-wave and $T=\frac{1}{2}$ p-wave phase shifts. For the other type, the signs of the phase shifts are almost all reversed. Each type consists of a pair of solutions which are intrinsically indistinguishable at low energies because of the impossibility of determining the sign of the spin-flip scattering amplitude. A choice between the two types of solution is in principle possible with improved data. Predictions of the angular distributions of π^- elastic scattering are made.

I. INTRODUCTION

THE study of the scattering of pi mesons from nucleons is one of the more direct means of investigating the meson-nucleon interaction. In this connection, the simplification introduced into the interpretation of meson-nucleon scattering by the hypothesis of charge independence is of current interest. This hypothesis allows one to describe all meson-nucleon scattering processes by specifying only $2(2l+1)$ phase shifts, where l is the largest relevant orbital quantum number of the incident meson. In the energy range in which the meson wavelength is more than its Compton wavelength, it is reasonable to limit consideration to low angular momentum states, $l=0$ and 1; one therefore seeks a measure of six phase shifts.

Angell, Perry, and Barnes *et al.*[1–3] have reported on the elastic-scattering processes at an incident energy of 37 Mev, and we have previously reported[4] a measurement of the total cross section for charge-exchange scattering at a mean energy of 34 Mev. In the present paper, we present the results[5] of a measurement of the angular distribution of charge-exchange scattering at a mean energy of 40 Mev. Within the experimental errors, all of these observations can be explained in terms of the same phase shifts.

II. METHOD

In previous observations[6–8] of the angular distribution of pion-proton charge-exchange scattering, only

* This work was supported in part by the U. S. Atomic Energy Commission.

[1] C. E. Angell and J. P. Perry, Phys. Rev. **92**, 835 (1953).

[2] J. P. Perry and C. E. Angell, Phys. Rev. **91**, 1289 (1953). J. P. Perry, thesis, University of Rochester, 1953 (unpublished).

[3] Barnes, Angell, Perry, Miller, and Nelson, Phys. Rev. **92**, 1327 (1953).

[4] A. Roberts and J. Tinlot, Phys. Rev. **90**, 951 (1953).

[5] A brief report of these results was presented at the 1954 New York meeting of the American Physical Society [Phys. Rev. **94**, 766 (1954)].

[6] Anderson, Fermi, Martin, and Nagle, Phys. Rev. **91**, 155 (1953).

[7] Fermi, Glicksman, Martin, and Nagle, Phys. Rev. **92**, 161 (1953).

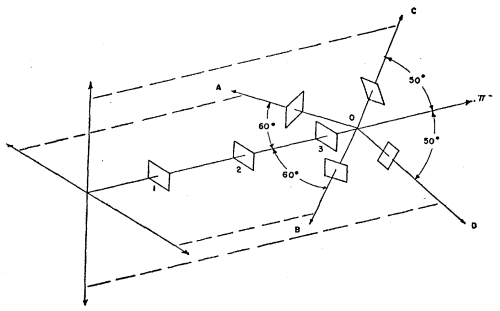

FIG. 1. Arrangement of photon detectors A, B, C, D in approximate tetrahedral geometry.

one of the two π^0 decay photons was detected. At the π^- energies involved in these experiments (60 Mev and above), a fairly strong correlation exists between the angular distributions of the photons and of the parent π^0 mesons. At 40 Mev, this correlation is very weak; therefore, it becomes necessary to detect both photons to obtain the π^0 angular distribution with reasonable accuracy.

The usable intensity of π^- mesons in our experiment was such ($\sim$1000 min^{-1} cm^{-2}) that the rate of counting charge-exchange events by observing two coincident photons was expected to be very low—of the order of 4 counts per hour—even though the photon detectors subtended rather large solid angles at the target. Thus, simultaneous measurements at several π^0 emission directions were clearly desirable. Accordingly, we took advantage of a peculiarity of π^0 decay kinematics. At the average π^- energy of 40 Mev, the minimum (and most probable) angle between the two decay photons has a value of about 110°, averaged over the range of π^0 energies. This angle is very nearly the same as that between the axes of symmetry of a regular tetrahedron (109° 28′). For this reason, four photon detectors were placed so that their axes coincided approximately with those of an imaginary tetrahedron[9] centered on the target. (See Fig. 1.) In the resulting assembly, one pair of detectors (C and D) counted neutral mesons emitted predominantly in the forward direction; another pair (A and B) those emitted backward; and the four other pairs (A, C; A, D; B, C; B, D) those emitted near 90°. The symmetry of the detectors is that of the point group C_{2v}; i.e., there is a twofold axis of symmetry and two mutually perpendicular planes of symmetry containing this axis, as in the molecule CH_2Cl_2. Since there can be no azimuthal angular dependence, the four 90° pairs are essentially identical.

The terms "backward," "forward," and "90°" are only very approximate designations of the angular definition of the detector pairs. It will be seen (Fig. 2) that each pair of detectors is sensitive over an angular range exceeding 90°.

III. APPARATUS AND PROCEDURE

(a) Experimental Arrangement

The π^- beam used in this experiment was the external 50-Mev beam of the Rochester synchrocyclotron, selected in energy and focused by the cyclotron fringing field, a "z-focusing" magnet, and a double-focusing wedge magnet. The general arrangement is shown in Fig. 3. The resulting beam traversed a counter telescope (counters 1, 2, 3) consisting of scintillators 2 in.$\times$2 in. $\times\frac{3}{16}$ in., and entered the target. A fourth scintillator (4), having the form of a hollow rectangular box open on one side, surrounded the target, as indicated in Fig. 4b. Counter 4 was in anticoincidence with the meson telescope counters and served to eliminate mesons which traversed the target without interacting,

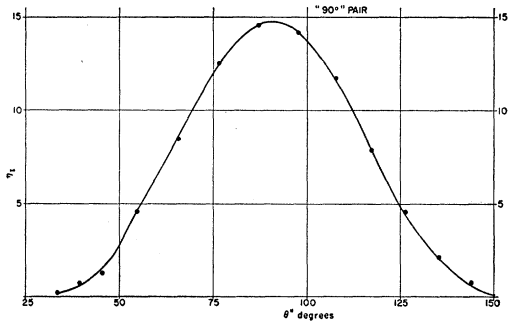

FIG. 2. The relative efficiency of a 90° pair of counters for detecting a neutral meson, as a function of angle of emission in the c.m. system.

or which produced ionizing fragments by interaction in nonhydrogenous material. Mesons elastically scattered from target nuclei could not penetrate the photon detectors, and therefore were not counted. Each of four photon detectors consisted of a $\frac{1}{4}$-in. Pb converter in front of two liquid scintillators, the first of which had dimensions 3.5 in.$\times$3.5 in.$\times$0.9 in., and the second, 4 in.$\times$4 in.$\times$0.4 in.; the two counters were separated by $\frac{1}{16}$ in. aluminum (see Fig. 4a). An 8-Mev electron could just penetrate the counters and aluminum. This threshold energy was selected to simplify the calculation of photon detection efficiency.[10]

(b) Targets

The targets used were either CH_2 or C, and had square cross sections $2\frac{1}{4}$ in.$\times 2\frac{1}{4}$ in.

The hydrogen effect was determined by taking CH_2-C differences. Approximately equal amounts of

[8] Bodansky, Sachs, and Steinberger, Nevis Cyclotron Laboratories Report No. 1, 1953, Phys. Rev. **93**, 1367 (1954).

[9] The regular tetrahedron geometry would be suitable in the meson-proton center-of-mass system. In order to compensate roughly for the center-of-mass motion (which causes forward photon pairs to have smaller angular separation than backward ones), the axes chosen were slightly distorted from those of the tetrahedron.

[10] The same criterion was used in the experiment of reference 4, and is discussed in more detail there.

data were taken using targets of equal stopping power, and targets of equal carbon content. In the first case, the surface densities of CH_2 and C were 2.06 g-cm^{-2} and 2.50 g-cm^{-2}, respectively; in the second case the CH_2 surface density was 2.92 g-cm^{-2}, and the carbon target was unchanged. The meson energy spread was 34 to 43 Mev in the "thin" CH_2 and carbon targets, and 29 to 43 Mev in the "thick" CH_2 target. In order to obtain the mean interaction energy, we weight the meson energy as a function of depth by the total cross section, as measured by Spry.[11] The mean meson energy in the "thin" CH_2 target is 40 Mev. Although the mean meson energy in the "thick" CH_2 target is somewhat lower, the results from the two target thickness can be combined, if one assumes slow variation of the angular distribution at this energy. As shown in Sec. V and VI, this is a reasonable assumption.

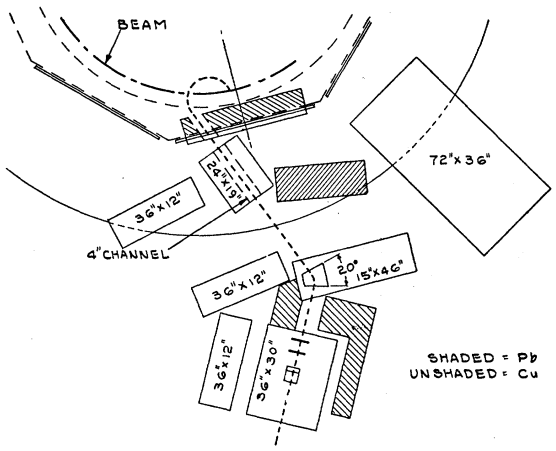

FIG. 3. Arrangement of apparatus at the cyclotron, showing the focusing magnets and some of the shielding.

(c) Shielding

The mechanical assembly of the twelve scintillators and associated photomultipliers (seven 1P21, four 6199, and one 6292) was greatly facilitated by using only enough iron and Permalloy to shield the multipliers against fields of the order of 5 to 10 gauss, instead of the 100–200 gauss cyclotron fringing field. The entire array was mounted inside the rectangular H yoke of a large magnet originally intended for cloud-chamber use; the sides of the yoke were closed with 2-in. iron plates. A 3-in. hole in one end of the yoke collimated the meson beam. The yoke served both as an adequate magnetic shield and as a shield against cyclotron radiation.

(d) Electronics

A simplified block diagram of the circuits used is shown in Fig. 5. The meson telescope triples and the anticoincidence rate ($123\bar{4}$), which will be called M, were recorded. Coincidences MA, MB, MC, and MD

[11] W. Spry, Phys. Rev. **94**, 766 (1954).

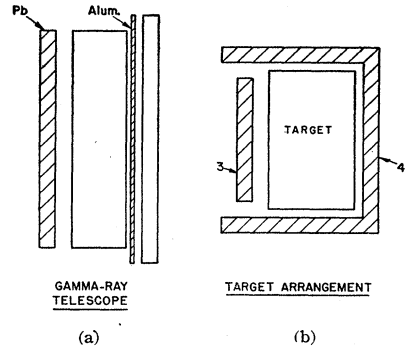

FIG. 4. (a) Detail of gamma-ray detector, showing lead converter, two liquid scintillators, and aluminum absorber between them. (b) Detail of target arrangement inside the hollow anticoincidence counter, No. 4.

of M with each photon detector were formed in a fast (20 mμsec) and a slow (0.1 μsec) circuit. The data from the slow circuit (with one input delayed) were used to compute accidental rates. The CH_2-C differences in the fast rates, after correction for accidentals, are a measure of the single photon yield from hydrogen. The results were useful as a continuing check on the operation of the photon detectors. The coincident photon rates $MAB\cdots MCD$ were obtained by forming coincidences between the six combinations of counts $MA\cdots MD$ in separate coincidence circuits. This scheme was chosen because it served to define resolving times and required relatively slow final coincidence circuits. The accidental background in the $MAB\cdots MCD$ rates was negligible. In view of the complexity of the circuitry and the low counting rates, independent instrumental checks were obtained in the following ways:

(1) A triple coincidence between M and any two photon detectors (called MXY) was formed in a combination coincidence and addition circuit. These counts were recorded directly, and also in coincidence with a 500-μsec gate which included the total time of the beam on target (about 250 μsec).

(2) The rates $MA\cdots MD$, $MAB\cdots MCD$, MXY, and gated MXY were recorded in register circuits and

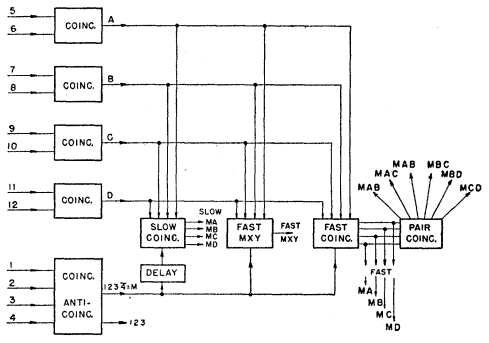

FIG. 5. Simplified block diagram of the circuits used. Not shown are the beam gating circuit and 20-channel pen recorder (see text), and sundry amplifiers, discriminators, pulse equalizers, etc.

on a 20-channel Esterline-Angus pen recorder. An analysis of the pen-recorder chart was expected to show that, for example, each MBC count was accompanied by MXY, gated MXY, MB, and MC counts. A few spurious counts were eliminated by applying this criterion.

All coincidence circuits were of the general type described by Garwin.[12]

(e) Counter Checks

It was thought advisable to calibrate the absolute efficiency of the individual photon detectors for counting single minimum-ionization particles, both before and after obtaining data. For this purpose, we used the 15 percent electron contamination in the negative meson beam. Since the electrons have the same momentum as do the mesons (130 Mev/c), their range is much greater than that of either π or μ mesons. The mesons were stopped by interposing about 2 in. of CH_2 and C. Each photon telescope was then placed between counter 3 and counter 4 (after the latter had been retracted), and the efficiency of the telescope measured by taking the ratio of 6-fold to 4-fold coincidences. The efficiencies were found to be about 90 percent. We consider this appreciable counting loss to be explained, at least in part, by the poor light collection from the large counters, particularly those viewed by 1P21 multipliers. We believe, however, that the resulting inefficiency for counting π^0-decay photons is quite negligible. The reason is that, according to Wilson,[13] the most probable numbers of conversion electrons produced in $\frac{1}{4}$ in. of Pb by a photon of energy near 100 Mev are zero or two; the probability of producing only one electron of energy greater than 8 Mev is less than 10 percent. (This is because the major interaction is pair production.) The counter efficiency for the detection of a converted high-energy photon should therefore be near 100 percent.

IV. GEOMETRICAL CALIBRATION OF THE APPARATUS

The calculation of the angular definition and effective solid angles for π^0 detection involves a number of lengthy computations. Since none of the usual small-angle approximations can be applied, we have used a procedure which allows us, in principle, to deduce the probability of detecting π^0 mesons emitted with an arbitrary angular distribution. For each pair of photon detectors, we compute the probability function $\bar{I}(\theta)d\theta$ which is the probability of detecting a π^0 meson emitted at angle θ in $d\theta$. This function is then transformed to the corresponding function $\bar{I}^*(\theta^*)$ in the meson-proton center-of-mass system. If we consider only the effects of s- and p-wave scattering, the π^0 angular distribution will have the form

$$J(\theta^*)=a+b\cos\theta^*+c\cos^2\theta^*, \tag{1}$$

and the probability η_i of detecting a π^0 meson in the ith pair of detectors will be

$$\eta_i=a\eta_{i1}+b\eta_{i2}+c\eta_{i3}=[4\pi(a+c/3)]^{-1}\int_0^{\pi}\langle\bar{I}^*(\theta^*)\rangle_{\mathrm{Av}} \times(a+b\cos\theta^*+c\cos^2\theta^*)\sin\theta^*d\theta^*. \tag{2}$$

This expression is normalized to a π^0 flux of unity. The ratio R_i of detected π^0 to incident π^- mesons is then the product of η_i and the probability of production of a π^0 meson:

$$R_i=(a\eta_{i1}+b\eta_{i2}+c\eta_{i3})\kappa\rho N\sigma_t x, \tag{3}$$

in which formula ρ is the fraction of π^- mesons in the impure "meson" beam, σ_t is the total charge exchange cross section, κ is a correction factor for gamma-ray detector losses, N is Avogadro's number, and x is the target surface density. σ_t can be eliminated by using the relation

$$\sigma_t=4\pi(a+c/3), \tag{4}$$

and a, b, and c expressed as differential cross sections. With three equations like (3), corresponding to detection in the forward, 90°, and backward pairs of detectors, we can solve for a, b, and c.

(a) Calculation of $\bar{I}(\theta)$

In the following paragraphs, we shall make frequent reference to the geometry of the experiment, as illustrated in Fig. 6. Suppose that a π^--meson incident along the Z axis interacts with a proton, and a π^0 meson is emitted in a direction specified by θ and ϕ. The meson decays essentially at the point of origin into two photons whose directions of flight lie in a plane containing the π^0 direction. The orientation of the plane is specified by the angle ϕ' with an arbitrary reference plane (since all values of ϕ' are equally probable). Let us define ξ as the angle between the two photon directions, and ζ as the inclination of one of them from the π^0 direction.

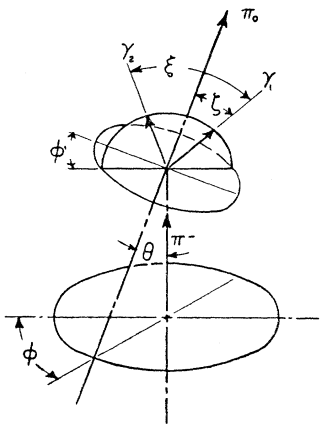

FIG. 6. Geometry of charge-exchange scattering. θ, ϕ are polar coordinates of the direction of the emitted π^0 meson. The plane of the two decay gamma rays is specified by ϕ', the angle between them by ξ, and the angle one gamma ray makes with the π^0 direction by ζ.

[12] R. L. Garwin, Rev. Sci. Instr. **21**, 569 (1950); Phys. Rev. **90**, 274 (1953).
[13] R. R. Wilson, Phys. Rev. **86**, 261 (1953).

The probability λ of detecting an event defined by the angles θ, ϕ, ξ, and $\zeta(\xi)$ is then equal to the probability that the photons strike two of the photon detectors, multiplied by the product of the intrinsic efficiencies ϵ_1 and ϵ_2 of the detectors. ϵ_1 and ϵ_2 depend on the photon energies, and therefore on the π^- energy and the angles θ, ξ. The probability that both photons strike the detectors is simply the fraction of 360° occupied by the range of ϕ' over which such space coincidence occurs. The quantity $I(\theta)$ is obtained by taking an appropriate average of λ over the variables ξ, ϕ; and $\bar{I}(\theta)$ by taking the average of $I(\theta)$ over the π^0 source position in the target. The procedure outlined above is done in the following sequence:

(1) We first compute the energy of the π^0 meson in the laboratory system for various values of θ, for π^- energies appropriate to the source positions in the target.

(2) For each value of the π^0-meson energy, we evaluate the differential correlation probability $P(\xi)d\xi$ that the angle ξ between the two photon directions lies in the range $d\xi$, and calculate the related values of ζ.

(3) We then determine the effective fractional range of ϕ' for space coincidence at a number of values of ξ, holding θ and ϕ fixed. The measurement is then repeated over the entire range of θ and ϕ.

(4) The numbers obtained in part (3) are multiplied by the corresponding product of detection efficiencies $\epsilon_1\epsilon_2$, weighted by the correlation probability $P(\xi)$, and averaged over the range of ξ.

(5) The results of steps 3 and 4 are then averaged over ϕ for each value of θ. This gives $I(\theta)$, the detection probability for a given value of θ.

(6) Finally, we repeat the procedure of steps (3), (4), and (5) for a selected number of source points in the target, and obtain a weighted average over the target. The result is the quantity $\bar{I}(\theta)$.

(7) The transformed function $\bar{I}^*(\theta^*)$ is calculated; we neglect the small variation in center-of-mass motion because of the distribution in π^- interaction energy, and transform to the system corresponding to the average interaction energy. The resulting function $\bar{I}^*(\theta^*)$ appears in Eq. (2) for the detection efficiency. The calculations in steps (1) and (2) of the above procedure involve straightforward application of the formulas for π^0 kinematics,[14] which for convenience are given in the appendix.

In performing step (4), we have, as in our previous work, used the Monte Carlo calculations of Wilson[13] to evaluate the intrinsic photon detection efficiency ϵ as a function of photon energy.

The results of steps (3)–(6) are peculiar to the experimental arrangement, and could in principle be obtained analytically. Preliminary study showed that an analytical solution would require a prohibitive effort. Accordingly, we adopted a numerical sampling method involving the use of a simple mechanical device (actually an analog computer) as an aid in performing these operations.

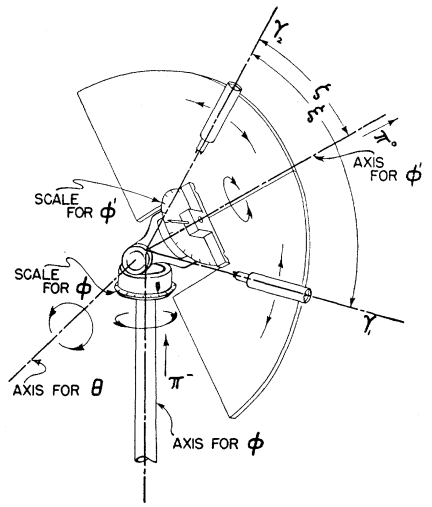

FIG. 7. The analog computer used for solid angle determinations. The angles shown are those defined in Fig. 6.

(b) The Analog Computer

The analog computer was constructed to duplicate the geometry of Fig. 6, on a scale three times actual size, with rectangular screens representing the photon detectors. A drawing of the computer is shown in Fig. 7. A swivel camera mount was modified to hold a semicircular plate, which supported two flashlights with collimated light beams. The movable axis of the mount, representing the direction of the π^0 meson, could be oriented over a wide range of directions (specified by θ and ϕ), and the plane of the light beams rotated about this axis; the relative angular position of the plane represented the variable ϕ'. The light beams were directed from the center of rotation of the mount and were inclined from the axis by angles ζ and $\xi-\zeta$. To implement the procedure of step (3), we then (a) set the center of the mount at a position corresponding to a chosen point in the target, (b) adjust the coordinates of the movable axis to particular values of θ, ϕ, (c) set the flashlight beams at appropriate angles ζ, $\xi-\zeta$, as determined in step (2), and (d) measure the range of ϕ' over which the light beams strike the two screens.

Data were obtained in this way for θ taken in 5° steps and ϕ in 30° steps in the cases of the backward and forward pairs of detectors, and for θ and ϕ both in steps of 10° for the 90° pairs. In most cases, 4 sets of values of ζ and $\xi-\zeta$ were taken for each position of the mount. It was shown that this sampling was adequate by repeating some of the measurements for seven sets of values for ζ and $\xi-\zeta$. The entire procedure was carried out for seven different source points in the

[14] Some of these are given by J. Steinberger and A. S. Bishop, Phys. Rev. **86**, 171 (1952); Panofsky, Steinberger, and Steller, Phys. Rev. **86**, 180 (1952).

TABLE I. Observed numbers of gamma-gamma coincidences.

Target	No. of 123 coinc. $\times 10^{-6}$	Total counts in pair: AB (180°)	AC (90°)	AD (90°)	BC (90°)	BD (90°)	CD (0°)
None	5.0	10	1	1	0	4	0
Carbon	10.03	30	9	7	14	10	3
2.92 g/cm² CH_2	12.3	99	41	41	32	40	6
2.06 g/cm² CH_2	20.4	134	56	54	45	47	6
CH_2, C, no Pb conv.	2.0	1	0	1	1	0	0

TABLE II. Counts per million 123 triples. The 90° pairs have been averaged.

Target	180°	90°	0°
A. None	2.0 ±0.7	0.3 ±0.15	0
B. Carbon	3.00±0.55	1.00±0.16	0.30±0.17
C. "Thick" CH_2	8.05±0.80	3.12±0.25	0.49±0.25
D. "Thin" CH_2	6.55±0.56	2.50±0.16	0.29±0.12

target: the center of the target and the centers of the six faces. The results were then averaged using Simpson's rule for numerical integration. Figure 2 shows the result for the "90°" pairs.

It is of course very difficult to estimate the error in $\bar{I}(\theta)$ arising from observational errors, insufficient sampling, and uncertainties in Wilson's shower theory. We believe, however, that although the uncertainly in $\bar{I}(\theta)$ may be quite large for some values of θ, the resulting relative uncertainties in the detection efficiencies η_i are probably not larger than 10 percent.

V. REDUCTION OF DATA

The individual total counts for all of the pairs of photon detectors are given in Table I, and the rates per million triple coincidences (123) are shown in Table II. The hydrogen effect (Table III) was determined in different ways for the two CH_2 targets. It is simply the CH_2-C difference in the case of the "thick" CH_2 target (equal carbon content). In the case of the thin CH_2 target, we must take into account the yield with no target. If σ is the ratio of carbon nuclei in the CH_2 and C targets, then

$$\text{Hydrogen yield} = (CH_2 \text{ yield}) - \sigma(\text{C yield}) - (1-\sigma)(\text{no target yield}).$$

The results for the two different targets were in excellent agreement for all pairs of detectors, if account was taken of the slight reduction in total cross section in the energy range 29–34 Mev, compared to 34–43 Mev. Therefore, the hydrogen effects obtained with both targets have been averaged in Table III. It will be seen that, within statistics, the four 90° pairs gave equal rates; this is to be expected, since the counter array has the above-mentioned C_{2v} symmetry about the incident π^- direction. It should also be noted that the rates with no Pb converters are very low; this result is a strong indication that (a) the phenomenon we have observed is truly the consequence of coincident photons, and (b) the accidental counting rates are negligibly small. The individual rates $MA\cdots MD$ are not given, but were in all cases equal within the experimental errors. The factor κ in Eq. (3) includes several corrections which must be applied to the data.

(a) The meson beam is attenuated by nuclear absorption in traversing the target, so that the number of 123 triples exceeds the number of effective mesons in the target. We estimate this correction as one percent.

(b) Each neutral meson decay gamma ray has a 0.7 percent probability of being internally converted;[15] if it is, counter 4 will prevent its being recorded. The correction for two gamma rays in coincidence is thus 1.4 percent.

(c) The gamma rays may be converted in the target itself or in counter 4. An accurate estimate of this effect is difficult to make because of the wide variation in path lengths in the target. We estimate 3 percent probability of conversion for each gamma ray, or 6±2 percent for both.

(d) A few π^- mesons stop in the target and are captured in hydrogen; half of these captures result in π^0 emission yielding two gamma rays. A direct measurement of this process, made by stopping the entire beam in the target, gave a two-photon coincidence rate only three times that observed with fast π^-'s. We estimate this correction as not more than one percent, and have neglected it.

The radiative capture of π^- mesons produces only one gamma ray, and is therefore not observed.

Combining all the above corrections, we find a value for κ of 0.92±0.02.

VI. CALCULATION OF ANGULAR DISTRIBUTION

As stated previously, we assume that only *s*- and *p*-wave scatterings are important at this interaction energy. Accordingly, the equations obtained in Sec. IV for the detection efficiencies are directly applicable. Substitution of the results of Table III gives the following numerical relations (with $\rho=0.72$, $\kappa=0.92$,

TABLE III. Net hydrogen and carbon effects, in counts per million 123 triples.

Datum from Table II[a]	180°	90°	0°
$C-B$	5.05±0.97	2.12±0.30	0.19±0.30
$D-0.7B-0.3A$	3.85±0.70	1.70±0.20	0.09±0.17
Average H effect	3.94±0.52	1.70±0.16	0.11±0.15
Carbon effect $(B-A)$	1.0 ±0.9	0.70±0.23	0.3 ±0.2

[a] In Table II the targets of entries *B* and *C* contain the same number of C atoms; the first entry in Table III, $C-B$, is thus the net hydrogen effect for the "thick" CH_2 target. The second entry is the hydrogen effect for the "thin" CH_2 target, containing 0.7 as many C atoms. The average in the third line is normalized to the "thin" CH_2 target, assuming the total cross section at 29–33 Mev is 0.8 times the cross section from 33–43 Mev. (See reference 11.)

[15] Lindenfeld, Sachs, and Steinberger, Phys. Rev. **89**, 531 (1953).

$x=0.294$ g/cm^2):

$$\begin{aligned}(0°):&\quad 0.117(39.3a+31.7b+26.6c) &&=0.11\pm0.15,\\ (90°):&\quad 0.117(26.5a-0.69b+3.42c) &&=1.70\pm0.23,\\ (180°):&\quad 0.117(19.25a-16.9b+15.1c) &&=3.94\pm0.65,\end{aligned} \quad (5)$$

where a, b, and c are now in mb/sterad. The coefficients of a, b, and c are 10^3 times the values of η_1, η_2, and η_3 in Eq. (2). The errors in the counting ratios on the right-hand sides of the equations have been increased over those shown in Table III to take into account the uncertainty in the analog computations and in κ.

The solution of these equations gives the following angular distribution:

$$d\sigma^0/d\Omega=(0.45\pm0.07)-(0.98\pm0.13)\cos\theta +(0.54\pm0.21)\cos^2\theta \text{ mb/sterad}. \quad (6)$$

This distribution is strongly peaked in the backward direction, in agreement with results[6–8] at higher energies. From Eq. (4), the total cross section is found to be $\sigma_t=7.9\pm1.8$ mb, where an estimated additional error in absolute gamma-ray efficiency has been added. This number is in reasonable agreement with our previous result[3] at 34 Mev (5.5 ± 1.5 mb), assuming the angular distribution given above, and with the more recent measurements of Spry[11] (6.9 ± 1.2 mb at 42 Mev).

VII. ANALYSIS AND DISCUSSION OF RESULTS

(a) Evaluation of Phase Shifts

The analysis of pion-nucleon scattering is usually carried out according to the hypothesis of charge independence. Accordingly, if only s- and p-wave scattering contribute, there are six independent phase shifts, corresponding to the combinations $l=0$ or 1, $J=1\pm\frac{1}{2}$, and $T=\frac{1}{2}$ or $\frac{3}{2}$. They are conventionally denoted by α_{ij}, where $i=2T$, $j=2J$ (but is omitted for $l=0$). These six phase shifts, in suitable combinations, should describe the scattering of pions of any sort by either neutrons or protons.

The expressions of Van Hove,[16] in which the first order Coulomb terms are retained, can be written as follows for the observable cases:

$$\frac{d\sigma^+}{d\Omega}=\frac{1}{k^2}\left[\left(x_+ + y_+\cos\theta-\frac{\alpha}{2\sin^2(\theta/2)}\right)^2+z_+^2\sin^2\theta\right], \quad (7)$$

$$\frac{d\sigma^-}{d\Omega}=\frac{1}{9k^2}\left[\left(x_- + y_-\cos\theta+\frac{3\alpha}{2\sin^2(\theta/2)}\right)^2+z_-^2\sin^2\theta\right], \quad (8)$$

$$\frac{d\sigma^0}{d\Omega}=\frac{2}{9k^2}\frac{v_0}{v}[(x_0+y_0\cos\theta)^2+z_0^2\sin^2\theta]. \quad (9)$$

In Eqs. (7) and (8), which refer to elastic scattering from protons, α is a relativistic Coulomb phase shift discussed by Van Hove. In Eq. (9), which describes charge-exchange scattering from protons, we have inserted the factor v_0/v which is usually omitted. Here v_0 is the velocity of the neutral meson relative to the neutron, and v that of the charged meson relative to the proton. The factor v_0/v (which differs appreciably from unity only at low energies) arises from the definition of flux for the charge-exchange process, which in reality is an exothermic reaction. At 40 Mev, the value of v_0/v is 1.05. The coefficients x, y, and z are directly related to the s- and p-wave phase shifts. Their values in the small angle approximation which we adopt [$\exp(2i\alpha)-1\approx 2i\alpha$] are shown in Table IV.

[16] L. Van Hove, Phys. Rev. **88**, 1358 (1952).

TABLE IV. Relations between scattering parameters and phase shifts, in the small-angle approximation.

Scattering process	x	y	z
+	α_3	k	m
−	$\alpha_3+2\alpha_1$	$k+2l$	$m+2n$
0	$\alpha_3-\alpha_1$	$k-l$	$m-n$

$k=2\alpha_{33}+\alpha_{31}$, $l=2\alpha_{13}+\alpha_{11}$, $m=\alpha_{33}-\alpha_{31}$, $n=\alpha_{13}-\alpha_{11}$.

It is convenient to write the experimental angular distribution for charge exchange scattering in the form

$$\frac{d\sigma^0}{d\Omega}=\frac{2}{9k^2}\frac{v_0}{v}(A+B\cos\theta+C\cos^2\theta), \quad (10)$$

and to define new parameters,

$$\mu=(A+B+C)^{\frac{1}{2}},\quad \lambda=(A-B+C)^{\frac{1}{2}}. \quad (11)$$

Combining Eqs. (9), (10), and (11), we obtain the following solutions for the parameters x_0, y_0, and z_0;

$$\begin{aligned}&x_0=\tfrac{1}{2}(\mu+\lambda),\quad y_0=\tfrac{1}{2}(\mu-\lambda),\quad z_0^2=\tfrac{1}{2}(A-C-\mu\lambda),\\ &x_0=\tfrac{1}{2}(-\mu+\lambda),\quad y_0=\tfrac{1}{2}(-\mu-\lambda),\quad z_0^2=\tfrac{1}{2}(A-C+\mu\lambda),\\ &x_0=\tfrac{1}{2}(-\mu-\lambda),\quad y_0=\tfrac{1}{2}(\mu+\lambda),\quad z_0^2=\tfrac{1}{2}(A-C-\mu\lambda),\\ &x_0=\tfrac{1}{2}(\mu-\lambda),\quad y_0=\tfrac{1}{2}(-\mu+\lambda),\quad z_0^2=\tfrac{1}{2}(A-C+\mu\lambda).\end{aligned} \quad (12)$$

There are in reality eight separate solutions, since z_0 can be either positive or negative. Upon evaluating A, B, C, μ, and λ from the values given in Eq. (6), we find that $\mu=0$, and that $(A-C)$ is negative. The latter condition would require z_0 to be imaginary, which is inadmissible since imaginary phase shifts cannot represent a pure scattering process. Within the experimental uncertainty, it is quite possible to take $(A-C)$ to be zero, in which case there are only two distinct solutions:

$$x_0=\pm\tfrac{1}{2}\lambda=\pm0.22,\quad y_0=\mp\tfrac{1}{2}\lambda=\mp0.22,\quad z_0=0. \quad (13)$$

One should in principle be able to make a choice of signs from information as to the nature of the Coulomb interference in elastic scattering, and thus select a unique solution.

The above result is not necessarily the best fit to the data, and the uncertainties cannot be deduced in any

TABLE V. Acceptable solutions for phase-shift parameters of charge-exchange scattering. ω is the deviation parameter defined in the text. x_0, y_0, and z_0 are in radians, phase shifts in degrees.

Solution	x_0	y_0	z_0	x_0 $=\alpha_{33}-\alpha_{11}$	$\frac{1}{3}(y_0+z_0)$ $=\alpha_{33}-\alpha_{13}$	$\frac{1}{3}(y_0-2z_0)$ $=\alpha_{31}-\alpha_{11}$	ω
a	−0.21	0.24	0	−12.0°	4.6°	4.6°	0
b	0.21	−0.24	0	12.0	−4.6	−4.6	0
c	−0.17	0.28	0.14	−9.7	8.0	0	0.7
d	0.17	−0.28	0.14	9.7	−2.7	−10.7	0.7
e	−0.17	0.28	−0.14	−9.7	2.7	10.7	0.7
f	0.17	−0.28	−0.14	9.7	−8.0	0	0.7

simple way; furthermore, if one allows z_0^2 to have a positive value, as is quite possible within the errors, the degeneracy in the preceding solutions disappears. We have accordingly tried to fit the distribution of Eq. (6) with a number of values of the parameters x_0, y_0, and z_0, and computed the deviation from the experimental points by evaluating the quantity, $\omega=\sum_{i=1}^{3}(\delta_i^2/\Delta_i^2)$, where δ_i is the deviation of the predicted value from the observed value of the ith coefficient of the distribution, and Δ_i is the corresponding standard deviation in that coefficient. Assuming that $\omega\leqq 1.5$ defines a reasonable fit to the data, we find that acceptable solutions exist only for the values of z_0^2 between 0 and 0.03. The best values of x_0 and y_0 have been evaluated for $z_0^2=0$ and 0.02, and these results and the corresponding relations between the phase shifts appear in Table V. It may be noted that the value of ω for solutions *a* and *b* is essentially zero, indicating a perfect "fit."

(b) Comparison with Results of Elastic Scattering

The pairs of solutions *a*, *b*; *c*, *d*; and *e*, *f* correspond to opposite sign of spin-flip terms z_0; *c*, *f* comprise a "Fermi," *d*, *e*, a "Yang" pair. We now inquire as to which (if any) of these six sets can be discarded, from a comparison with the results on elastic scattering at about the same energy.

It is readily seen that no choice can ever be made between solutions differing only in the sign of z. Reversing the signs of m and n, as defined in Table IV, will obviously leave all angular distributions unchanged, since z only enters quadratically in Eqs. (7) to (9). (The individual phase shifts will in general be different in the two cases.) This conclusion is valid only at low energies, when the angles are so small that the approximate expressions of Table IV can be used. At higher energies, it may be possible to determine the sign of the spin-flip terms.

It may be hoped, however, that the results of the present experiment could be used to determine the sign of the interference term in Coulomb and nuclear scattering, and to test the hypothesis of charge independence. Since the present experiment yields only three relations among the six phase shifts, we have combined our results with those obtained from an analysis of the π^+ elastic scattering data of Perry and Angell.[3] These two experiments together give six conditions on the six phase shifts and therefore determine the possible values. The results can then be checked against the available data on π^- scattering.

A recalculation, including first-order Coulomb terms, of possible fits to the data of Perry and Angell is in progress;[17] preliminary results obtained by Noyes give two sets of scattering parameters (four sets of phase shifts, because of the spin-flip degeneracy) which fit the π^+ scattering data. Because of the limited accuracy of the data, rather wide variation of the parameters is possible. We have included in Table VI, which gives the scattering parameters for the π^+ data, the two "best" fits (solution 1–4) and a variant of each (solution 5–8).

It is now appropriate to try to fit the available π^- scattering data at 37 Mev, using combinations of solutions from Table V and VI. The available data[1,3] include the total π^- scattering cross section for angles larger than 55°, and the differential scattering cross section at 45° (laboratory angle).

From the total attenuation cross section (12.9±1.7 mb) and our measurement of the total charge exchange cross section (7.9±1.8 mb) we obtain a total elastic-scattering cross section of 5.0±2.5 mb. The 45° cross section has been measured to be 1.7±0.4 mb.

Comparison of the predicted values with the measured ones shows that there are three acceptable sets of scattering parameters; because of the spin-flip degeneracy, there are, thus, six allowed sets of phase shifts. These sets, and the corresponding predicted cross sections, are given in Table VII, and the predicted π^- elastic-scattering angular distributions are shown in Fig. 8. One of the allowed sets (labeled 7a in Table VII) is of the conventional "Fermi" type, and is nearly identical with that deduced by Perry and Angell—positive α_{33}, small negative α_3; set 8a is the corresponding "Yang" type solution. The other sets are basically different, in that α_3 is large and positive, the $T=\frac{3}{2}$ *p*-wave phase shifts are small and negative, and the $T=\frac{1}{2}$ *p*-wave phase shifts are quite large.

TABLE VI. Some possible parameters for 37-Mev π^+ angular distributions. x_+, y_+, z_+ are in radians, phase shifts in degrees. The deviation parameter in this case is $\omega=\sum_{i=1}^{5}\{[\sigma(\theta_i)-\sigma_{th}]^2/\Delta_i^2\}$. These parameters were deduced by Noyes from data of Perry and Angell (see reference 2).

Solution	x_+	y_+	z_+	α_3	α_{33}	α_{31}	ω
1	0.14	−0.09	−0.021	8.0°	−2.1°	−0.9°	0.3
2	0.14	−0.09	0.021	8.0	−1.3	−2.5	
3	−0.09	0.13	0.08	−5.2	4.0	−0.5	0.48
4	−0.09	0.13	−0.08	−5.2	1.0	5.5	
5	0.10	−0.15	−0.095	5.7	−4.7	0.7	0.9
6	0.10	−0.15	0.095	5.7	−1.0	−6.7	
7	−0.065	0.16	0.098	−3.7	4.9	−0.7	0.46
8	−0.065	0.16	−0.098	−3.7	1.2	6.8	

[17] We are indebted to H. P. Noyes for giving us the preliminary results of this investigation.

If we limit consideration to the conventional solutions (set III), we see that the conclusion of Barnes *et al.*[3] as to the relative sign of Coulomb and meson-nucleon forces is corroborated. A unique, but different, conclusion would be reached if one chose sets I and II, which correspond to solutions found at 65 and 78 Mev by Bodansky, Sachs, and Steinberger.[8] It may be that sets I and II cannot be extrapolated in a reasonable way to explain results at energies above 78 Mev; we have not investigated this question. It is possible that improved experimental results for elastic scattering will allow one to identify the correct set of solutions; the intrinsic spin-flip degeneracy will of course remain.

It should be noted that if one makes any reasonable extrapolation of the phase shifts for any of the solutions of Table V, the form of the charge-exchange distribution changes only slightly with energy in the range 30–50 Mev. It can therefore be concluded that the general results of the present experiment are not affected by the large spread in π^- interaction energy.

(c) Precision of Phase Shifts

It is difficult to assign uncertainties to the phase shifts given in Tables V and VI without making a much more thorough study of the experimental results for all three scattering processes. One should evidently evaluate the appropriate deviation parameter as a function of the six parameters α_1, α_3, k, l, m, n, taking into account all of the experimental points at 37–40 Mev. It is clear from the foregoing that we have not attempted this. We cannot therefore consider the sets of phase shifts of Tables V and VI to be true least-square fits but only representative values for the different acceptable types of solutions.

One can obtain qualitative indications as to the probable accuracy of the phase-shift determinations by noting how the phase shifts contribute to the scattering parameters (see Table IV). For example, the $p_{\frac{3}{2}}$ phase shifts contribute only to the parameters l and n. In turn, n enters into z_0 and z_-. Since z_0 must be very near zero, and enters quadratically in the expressions

TABLE VII. Pairs of solutions which fit π^- data: $\sigma^-(45°) \geqq 0.5$ mb/sterad and $\sigma_t^-(>55°)$ between 3 and 10 mb. Labeling of solutions follows that of Tables V and VI.

Set	Solution	$\sigma^-(45°)$ mb	$\sigma_t^-(>55°)$ mb	α_3	α_1	α_{33}	α_{31}	α_{13}	α_{11}
I	$1d$	1.0	5.8	8.0°	−1.7°	−2.1°	−0.9°	0.6°	9.8°
	$2f$			8.0	−1.7	−1.3	−2.5	6.7	−2.5
II	$1f$	0.78	3.0	8.0	−1.7	−2.1	−0.9	5.9	−0.9
	$2d$			8.0	−1.7	−1.3	−2.5	1.4	8.2
III	$7a$	0.8	6.7	−3.7	8.3	4.9	−0.7	0.3	−5.3
	$8a$			−3.7	8.3	1.2	6.8	−3.4	2.2
	$7a_1$ ($z_0=0.05$)			−3.7	8.3	4.9	−0.7	−0.6	−3.4
	$7a_2$ ($z_0=0.07$)			−3.7	8.3	4.9	−0.7	−1.0	−2.7
	$7a_3$ ($z_0=0.10$)			−3.7	8.3	4.9	−0.7	−1.5	−1.5

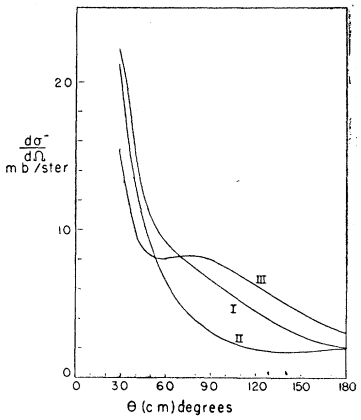

FIG. 8. Angular distributions of π^- elastic scattering predicted by the three solutions of Table VII. (Note: the ordinate scale should read 1.0, 2.0.... instead of 10, 20, ...)

for the differential cross sections, the $p_{\frac{3}{2}}$ phase shifts are particularly poorly determined by the charge-exchange results. For example, consider set $7a$ of Table VII, which corresponds to $z_0=0$, and gives α_{13} and α_{11} equal to 0.3° and −5.3°, respectively. Changing z_0^2 to 0.005 (which changes the angular distribution insignificantly) results in pairs of values for α_{13} and α_{11} of 1.6° and −7.9° (for $z_0=-0.07$) or −1.0 and −2.7° (for $z_0=+0.07$). A much larger variation in z_0 would be allowed if x_0 and y_0 were readjusted to give a best fit. Three variants on solution $7a$ are given at the end of Table VII. They show that the values of α_{13} and α_{11} are not well determined.

It should, however, be remarked that the angular distributions for π^- elastic scattering are strongly affected by these changes in z_0. The predicted distributions for solutions $7a$ to $7a_3$ give cross sections at 90° differing by almost a factor of 2.

The s and $p_{\frac{3}{2}}$ phase shifts appear in parameters whose values are more strictly defined and which enters in the scattering formulas in linear and quadratic combinations. From reasoning analogous to the foregoing, we believe that these phase shifts are determined to roughly 20 percent, within each set of Table VII.

VIII. ANOMALOUS EVENTS

In the course of the experiment, a total of 589 coincident photon events were recorded with a CH_2 target. In addition six cases of triple coincidences were recorded, all of which satisfied the rather rigid criteria outlined in Sec. III. No such events were observed during the runs with carbon target and no target, when three would have been expected if the effect were independent of target material. We have considered various hypotheses as to the origin of these events. These include the internal or external conversion in the target of one of the gamma rays (detection is suppressed by anticoincidence counter 4); backscattering of a shower electron in one lead radiator to count in another gamma-ray detector (too unlikely); three-photon decay of the neutral meson (forbidden by symmetry with

respect to charge conjugation[18]); detection of the neutron produced in charge-exchange in hydrogen (too improbable); interactions in carbon (threshold rather high, little energy left for gamma ray); and accidental coincidences (experimentally ruled out). A possibility which might be considered is the reaction $\pi^-+p\rightarrow\pi^0+n+h\nu$, which is one order in $e^2/\hbar c$ less likely than direct charge exchange. However, the available phase space is so small as to reduce the cross section another factor of 10^3. The possibility that the effect is instrumental cannot be ruled out. Further study by the means used in this experiment is rather impractical, in view of the counting rate of about one event in four hours.

IX. CHARGE EXCHANGE SCATTERING IN CARBON

Table III shows the net counting rate of coincident photons from carbon, as well as from hydrogen. Since charge-exchange scattering in carbon is not a unique two-body process, the energy distribution of the emitted neutral mesons is unknown. Accordingly the angular distribution and cross section cannot be inferred from the observed gamma-ray coincidence rates. It may be remarked, however, that the cross section for charge-exchange scattering in carbon seems to be less than that for hydrogen.

ACKNOWLEDGMENTS

We have been materially assisted in the construction of the complicated electronic circuitry by our chief electrical engineer, Kurt Enslein, and the Electronic Shop staff under L. Braun. We are indebted to Dr. E. M. Hafner and Mr. W. Chestnut, Mr. I. Goldberg, Mr. R. Harding, Mr. R. Santirocco, Mr. S. Spital, and Mr. W. Spry for assistance in the experimental work and in the laborious computations. We wish to acknowledge the cooperation of the laboratory staff in the design, construction, and setting up of the equipment, and we are indebted to Professor H. P. Noyes for discussions concerning the evaluation of the gamma-ray detector efficiencies, and the analysis of the π^+ data.

[18] L. Wolfenstein and D. G. Ravenhall, Phys. Rev. 88, 279 (1952).

APPENDIX

We summarize here, for convenience, the relations that govern the decay of a π^0 meson into two gamma rays.

Let the velocity of the meson be βc, its rest mass μ, its total energy $\gamma\mu$, and its direction the axis from which angles are measured. Let the angle between the two gamma rays be ξ, the angle one of them makes with the direction of the meson ζ, and their energies E_1 and E_2 (or in general E_γ).

Then the minimum angle $\xi_{\min}$ between the gamma rays is given by

$$\sin^2(\xi_{\min}/2)=1/\gamma^2,$$

and in general

$$\sin^2(\xi/2)=\mu^2/4E_1E_2.$$

If $P(\xi)d\xi$ is the probability that ξ lies between ξ and $\xi+d\xi$,

$$P(\xi)=\sin\xi/[\beta\gamma(1-\cos\xi)^{\frac{3}{2}}\{\gamma^2(1-\cos\xi)-2\}^{\frac{1}{2}}].$$

If we define

$$R=\int_{\xi_{\min}}^{\xi}P(\xi)d\xi$$

as the fraction of decays with ξ equal to or less than ξ, then

$$R=[\gamma^2-\csc^2(\xi/2)]^{\frac{1}{2}}(\beta\gamma)^{-1},$$
$$\cos\zeta=(\beta+R)(1+\beta R)^{-1},$$
$$\sin^2(\xi/2)=[\gamma^2+(1-\gamma^2)R^2]^{-1},$$
$$E_\gamma=\tfrac{1}{2}\mu\gamma(1\pm\beta R).$$